Solutions of Radiative Transfer for Nongray Gases within a 3-D Cylindrical Enclosure

Won-Hee Park*, Hyun-Sung Jung* and Tae-Kuk Kim**
Department of Mechanical engineering
Chung-Ang University, Huksuk-dong Dongjak-gu Seoul 156-756, Korea

Abstract

In multi-dimensional systems, various solution schemes for radiative transfer are suggested but the applicabilities and accuracies of these schemes have not yet fully tested due to the lack of reference solutions especially for nongray gases. In this paper we present some precise radiative transfer solutions for a black walled 3-dimensional cylindrical system filled with nongray gases having uniform temperature and concentration. The ray-tracing method with the T_N quadrature set and the SNB model are used to obtain the radiative transfer solutions by the nongray gases. The solutions presented in this paper are proved to be quite accurate and can be regarded as the reference solutions for the radiative transfer by nongray gases.

Key Word : Radiative Transfer Equation, SNB(Statistical Narrow Band) Model, Ray-Tracing Method, Nongray gas, TN quadrature set

Introduction

Radiative transfer in energy systems such as furnace, combustor, boiler and high temperature machinery is a significant mode of heat transfer. To analyze the radiative transfer in these systems, various solution schemes for the radiative transfer equation(RTE) in multi-dimensional enclosures were studied by many researchers. Most of recent computer simulations for the convection heat transfer with fluid dynamic problems are required to be performed in complicated three-dimensional configurations. Various modeling schemes of the radiative transfer within these multdimensional enclosures filled with participating media are available. Raithby and Chui[1] proposed the finite volume method (FVM) and Chui et. al[2] solved some three-dimensional problems by using the FVM. Cheung and Song[3] suggested the Discrete Ordinate Interpolation Method(DOIM) and Seo and Kim[4] and Cha and Song[5] applied the DOIM to the three dimensional enclosures. Maruyama and Aihara [6] suggested the radiation element method by the ray emission model(REM^2) and Maruyama and Aihara [7] applied the REM^2 to some arbitrary three dimensional shapes.

Although there are many schemes suggested for analysis of radiative transfer in multi-dimensional systems, the applicabilities and accuracies of these schemes have not yet fully tested for nongray gases. This is because the reference data for irregular multi-dimensional nongray gas radiation are very rare in the literature except for the result presented by Liu [8] and Kim et.al [9] for nongray gas within 3-D rectangular enclosures.

In this paper we present some precise radiative transfer solutions for a black walled 3-dimensional cylindrical system filled with nongray gases. The statistical narrow band (SNB)

* Graduate Student
** Professor
E-mail : kimtk@cau.ac.kr, TEL : 02-820-5282, FAX : 02-812-7851

model and the ray-tracing method with the TN quadrature set [10] are used for finding nongray solutions. The solutions obtained in this study are proved to be quite accurate and can be regarded as the exact solutions.

Basic Equations

Radiative Transfer Equation

The ray-traying method by Lockwood and Shah [11] solves the radiative transfer equation(RTE) by tracing the rays starting from the black walls to the point in the medium and/or on the black wall. The generalized spectral form of the RTE along a line of travel s from s_u to s_p in the Ω direction can be written as

$$I_{\lambda p}(s_p, \Omega) = I_{\lambda u}(s_u, \Omega) \exp\left(- \int_{s_u}^{s_p} \beta_\lambda(s)\, ds \right) + \int_{s_u}^{s_p} S_\lambda(s, \Omega) \exp\left(- \int_{s}^{s_p} \beta_\lambda(s')\, ds' \right) ds \tag{1}$$

The radiative source function appearing in Eq. (1) is expressed as

$$S_\lambda(s, \Omega) = a_\lambda(s) I_{\lambda b}(s) + \frac{\sigma_{s\lambda}(s)}{4\pi} \int_{4\pi} I_{\lambda p}(s, \Omega') \Phi_\lambda(\Omega ; \Omega')\, d\Omega' \tag{2}$$

where a_λ and $\sigma_{s\lambda}$ are the absorption and scattering coefficients of the medium respectively and they are related to the extinction coefficient, $\beta_\lambda = a_\lambda + \sigma_{s\lambda}$. Φ is the scattering phase function, and $I_{\lambda b}$ is the blackbody intensity of the medium at s.

For non-scattering(purely absorbing) media($\sigma_{s\lambda} = 0$), the RTE shown in Eqs. (1) and (2) are simplified as

$$I_{\lambda p}(s_p, \Omega) = I_{\lambda u}(s_u, \Omega) \exp\left(- \int_{s_u}^{s_p} a_\lambda(s)\, ds \right) + \int_{s_u}^{s_p} a_\lambda(s) I_{\lambda b}(s) \exp\left(- \int_{s}^{s_p} a_\lambda(s')\, ds' \right) ds \tag{3}$$

where the estimation point $s_p = (r_p, z_p)$ can be located on a wall or in the medium but the upstream point $s_u = (r_u, z_u)$, where the ray starts, is located on the black wall to trace a radiative ray as shown in Fig. 1.

For purely absorbing uniform media, we don't need the approximations such as the Curtis-Godson [12] or the Lindquist-Simmons [13] approximation The solution procedure by using Eq. (3) is effectively decoupled from the local effect. The exponential term in Eq. (3) is called the transmittance $\tau_\lambda(\Delta s)$ of the medium and is expressed for the uniform medium considered as

$$\tau_\lambda(\Delta s) = e^{-a_\lambda \Delta s} \tag{4}$$

where $\Delta s = s_p - s_u$ is the path length. By neglecting the change of $I_{\lambda b}$ within Δs, Eq. (3) can be expressed in a simpler form as

$$I_{\lambda p}(s_p, \Omega) = I_{\lambda u}(s_u, \Omega)\, \tau_\lambda(\Delta s) + I_{\lambda b}[1 - \tau_\lambda(\Delta s)] \tag{5}$$

Since the upstream point u is on the black surface ($I_{\lambda u} = I_{\lambda bw}$), Eq. (5) becomes

$$I_{\lambda p}(s_p, \Omega) = I_{\lambda bw}\, \tau_\lambda(\Delta s) + I_{\lambda b}[1 - \tau_\lambda(\Delta s)] \tag{6}$$

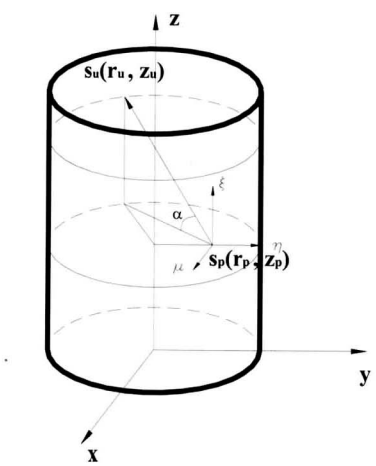

Fig. 1. Schematic diagram of the cylindrical enclosure.

Spectrally averaged RTE

If we want to apply a band approximation such as the narrow band model, a spectrally averaged form of Eq. (6) over a bandwidth $\Delta\lambda$ is needed.

$$\frac{1}{\Delta\lambda}\int_{\lambda_L}^{\lambda_U} I_{\lambda p}(s,\Omega)\,d\lambda = \frac{1}{\Delta\lambda}\int_{\lambda_L}^{\lambda_U} I_{\lambda bw}\tau_\lambda(\Delta s)\,d\lambda + \frac{1}{\Delta\lambda}\int_{\lambda_L}^{\lambda_U} I_{\lambda b}\,d\lambda - \frac{1}{\Delta\lambda}\int_{\lambda_L}^{\lambda_U} I_{\lambda b}\tau_\lambda(\Delta s)\,d\lambda \tag{7}$$

where $\lambda_U=\lambda+\Delta\lambda/2$ and $\lambda_L=\lambda-\Delta\lambda/2$.

Since the spectral dependency of the transmittance is very strong for most of the gases, we have to be careful in dealing with the spectral correlations between the transmittance and other variables [14]. The first and the last terms on the right hand side of Eq. (7) have this kind of spectral correlations. However, since the spectral variation of the blackbody intensity is relatively smooth as compared with the transmittance, the spectral correlation between the blackbody intensity and the transmittance is negligible. Then Eq. (7) can be approximated as

$$\frac{1}{\Delta\lambda}\int_{\lambda_L}^{\lambda_U} I_{\lambda p}(s,\Omega)\,d\lambda \fallingdotseq \frac{\sigma T_w^4}{\Delta\lambda}\int_{\lambda_L}^{\lambda_U}\frac{I_{\lambda bw}}{\sigma T_w^4}\,d\lambda\cdot\int_{\lambda_L}^{\lambda_U}\tau_\lambda(\Delta s)\,d\lambda + \frac{\sigma T_p^4}{\Delta\lambda}\int_{\lambda_L}^{\lambda_U}\frac{I_{\lambda b}}{\sigma T_p^4}\,d\lambda - \frac{\sigma T_p^4}{\Delta\lambda}\int_{\lambda_L}^{\lambda_U}\frac{I_{\lambda b}}{\sigma T_p^4}\,d\lambda\cdot\int_{\lambda_L}^{\lambda_U}\tau_\lambda(\Delta s)\,d\lambda \tag{8a}$$

fractions

$$\bar{I}_{\lambda p}(s_p) = \frac{\sigma T_p^4}{\Delta\lambda}F_{T_p\lambda_U-T_p\lambda_L} + \left[\sigma T_w^4 F_{T_w\lambda_U-T_w\lambda_L} - \sigma T_p^4 F_{T_p\lambda_U-T_p\lambda_L}\right]\cdot\bar{\tau}_\lambda(\Delta s) \tag{8b}$$

where $\bar{I}_{\lambda p}$, $\bar{\tau}_\lambda$ and $F_{T_p\lambda_U-T_p\lambda_L}$ are the band average intensity, the band average transmittance and the blackbody fraction over the band, respectively.

For a discrete direction $\Omega_m=(\mu,\xi,\eta)_m$, Eq. (8b) can be expressed by the following discrete form as

$$\bar{I}_{\lambda p,m}(s_{p,m}) = \frac{\sigma T_p^4}{\Delta\lambda}F_{T_p\lambda_U-T_p\lambda_L} + \left[\sigma T_w^4 F_{T_w\lambda_U-T_w\lambda_L} - \sigma T_p^4 F_{T_p\lambda_U-T_p\lambda_L}\right]\cdot\bar{\tau}_\lambda(\Delta s_m) \tag{9a}$$

where $m=1,\cdots,M$, where M is the number of discrete directions. The path length Δs_m is the distance between the two points, p and u, along the Ω_m direction as shown in Fig. 1. And T_p is the temperature of the gas or wall at point p.

For the k^{th} band, we may write it such that

$$\bar{I}_{k,p,m}(s_{p,m}) = \frac{\sigma T_p^4}{\Delta\lambda_k}F_{T_p\lambda_U-T_p\lambda_L} + \left[\sigma T_w^4 F_{T_w\lambda_U-T_w\lambda_L} - \sigma T_p^4 F_{T_p\lambda_U-T_p\lambda_L}\right]\cdot\bar{\tau}_\lambda(\Delta s_m) \tag{9b}$$

where $\Delta\lambda_k$ is the width of the k^{th} band.

Once the band average intensities for all K bands are obtained, the total intensity at point p is computed as

$$I_{p,m} = \sum_{k=1}^{K}\bar{I}_{k,p,m}\,\Delta\lambda_k \tag{10}$$

The radiative wall heat flux and the average intensity are computed with the radiative intensities obtained from Eq. (10) and they are represented by following dimensionless forms

$$Q_w^* = \frac{Q_w}{\sigma T_{hot}^4} = \frac{1}{\sigma T_{hot}^4} \sum_{m=1}^{M} I_{p,m} \eta_m w_m \tag{11}$$

$$G^* = \frac{\pi G}{\sigma T_{hot}^4} = \frac{1}{4\sigma T_{hot}^4} \sum_{m=1}^{M} I_{p,m} w_m \tag{12}$$

Statistical narrow band model

The statistical narrow band model was used to calculate the narrow band averaged gas transmittances. The narrow band averaged transmittance for isothermal and homogeneous gas along the pathlenth Δs is given by Ludwig [15].

$$\bar{\tau}(\Delta s) = \exp\left[-\frac{\overline{\beta_\nu}}{\pi} \left(\sqrt{(1 + \frac{2\pi f p \Delta s \overline{k_\nu}}{\overline{\beta_\nu}}} \right) \right] \tag{13}$$

where $\overline{k_\nu}$, $\overline{\beta_\nu}$ are the band averaged absorption coefficient and the line overlap parameter, respectively.

In this study, the SNB model parameters by Soufiani and Taine [16] were used. This data set covers the temperature range from $300K$ to $2900K$ and the spectral range from $150\,cm^{-1}$ to $9300\,cm^{-1}$ with a constant spectral interval $25cm^{-1}$.

Results

System configurations

The cylindrical enclosure considered in this study has the dimensions of $D=1m$ and $L=2m$. The normalized coordinates of $r^* = 2r/D$ and $z^* = z/L$ are used to present the results. All walls are assumed black and the bottom black wall is maintained at $T_{hot}=1000K$ and all the other walls are at $T_{cold}=0.5T_{hot}$. We considered two different medium temperature in cylinder. The first case is that the medium is at $T_g=0.5T_{hot}$ and the second case is that the medium temperature is at $T_g=0.7\,T_{hot}$.

The radiative wall heat flux is calculated on the side wall at $r^*=0.5$ along the z-axis, and the dimensionless average intensities are calculated along the center line of the cylinder(G_z^* at $r^*=0$) and along the r-axis at the half height(G_r^* at $z^*=0.5$), respectively. The numerical solutions are obtained at the specified r and z levels with 21 discrete points in both r- and z-directions. Since we are considering a uniform medium, the spatial diacretization does not affect the accuracy of the data, but the angular discretization plays a significant role for the accuracy. Therefore, we considered the T_{95} quadrature set[72200 angles (Thurgood et. al, 1995)] for the angular discretization. The typical CPU times spent for gray and nongray gas solutions using T_{95} quadrature set are about 10sec and 1500min, respectively, on Pentium Ⅳ 1.7GHz.

Gray gas solutions

Fig. 2 shows the dimensionless average intensity profiles(G_z^*) along the z-axis in the medium for different absorption coefficients. The T_{95} solution of the average intensity on the hot wall at $z^*=0$ is 0.53125 which coincides with the exact solution calculated using

$$G^*_{w,hot} = \frac{\pi G_{w,hot}}{\sigma T^4_{hot}} \int_{4\pi} I_p d\Omega$$
$$= \frac{1}{2T^4_{hot}} (T^4_{hot} + T^4_{cold}) \quad (14)$$
$$= 0.53125$$

Also the average intensity at the cold wall approaches the exact solution of 0.06250 as the optical depth increases. The average intensities shown in Fig. 2(a) decrease as the absorption coefficient increases due to the absorption by the cold medium. When the medium temperature is increased to $T_g = 0.7\,T_{hot}$, the average intensity profile along the z-axis shows a complicated change with the z coordinate. The average intensity increases on the hot wall, while it decreases near the bottom wall and increases again near the top cold wall as the absorption coefficient increases. This is due to the combined effects of the absorption and emission of the medium. Fig. 3 shows the dimensionless average intensity(G^*_r) along the r-axis at $z^* = 0.5$ for different absorption coefficients. The dimensionless average intensity near the mid point within medium approaches the exact value of 0.24010 as the optical depth increases.

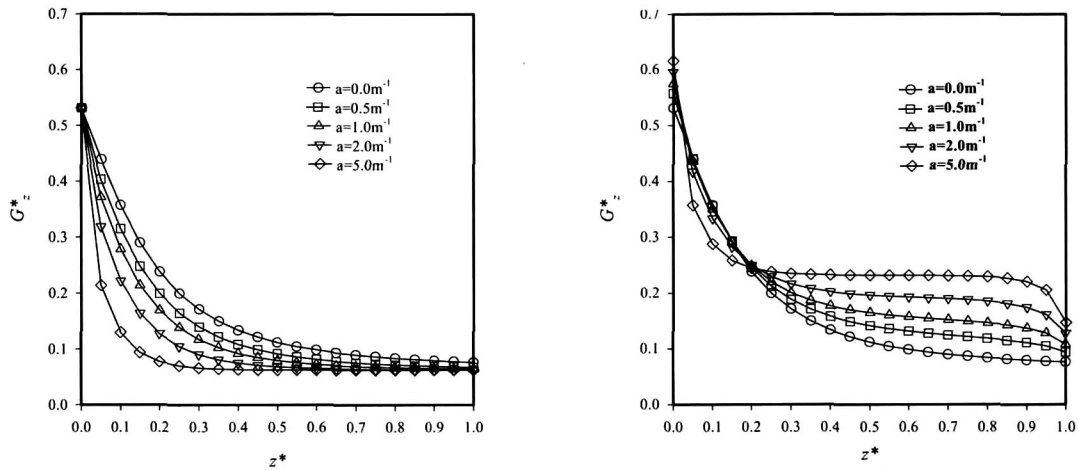

(a) $T_g = 0.5\,T_{hot}$ (b) $T_g = 0.7\,T_{hot}$

Fig. 2. Average intensity distributions for gray gases (G^*_z at $r^* = 0.0$).

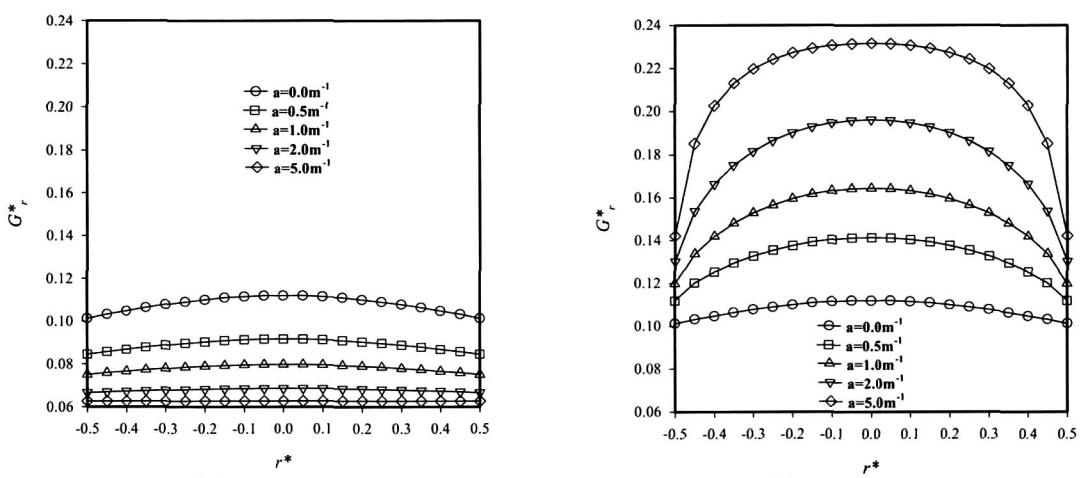

(a) $T_g = 0.5\,T_{hot}$ (b) $T_g = 0.7\,T_{hot}$

Fig. 3. Average intensity distributions for gray gases(G^*_r at $z^* = 0.5$).

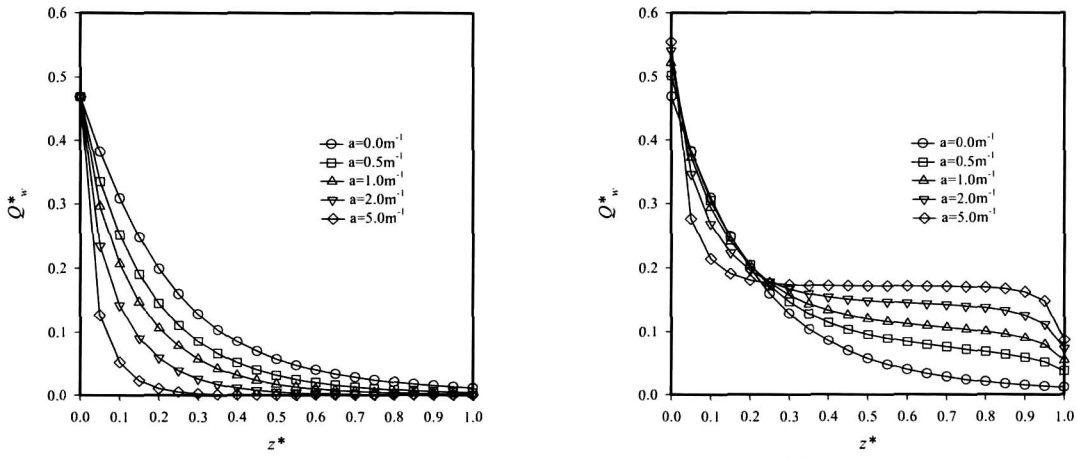

(a) $T_g = 0.5\,T_{hot}$ (b) $T_g = 0.7\,T_{hot}$

Fig. 4. Net side wall heat flux distributions for gray gases(Q^*_w at $r^* = 0.5$).

Fig. 4 shows the dimensionless net heat fluxes on the side wall along the z-axis for different absorption coefficients. For $T_g = 0.5T_{hot}$, the dimensionless radiative wall heat flux on the hot wall coincides with the exact value of 0.46875. The net side wall heat fluxes for $T_g = 0.5T_{hot}$ and $T_g = 0.7\,T_{hot}$ have similar trends to the average intensity profiles for the same medium temperatures.

Nongray gas solutions

Dimensionless average intensities and wall heat fluxes are obtained for nongray gases under the same conditions applied for gray gases. Fig. 5 shows the dimensionless average intensity(G^*_z) for different gas compositions at the center line of the cylinder along the z-axis. Since the H_2O gas absorbs more radiative energy than the CO_2 gas, the dimensionless average intensity increases as the medium contains more CO_2 for the low medium temperature of $T_g = 0.5T_{hot}$. But the dimensionless average intensity decreases near the cold bottom wall as the medium contains more CO_2 for the high medium temperature of $T_g = 0.7T_{hot}$. The dimensionless average intensity profiles along the r-axis at $z^* = 0.5$ (G^*_r) shown in Fig. 6 show these trends due to the change of the gas compositions.

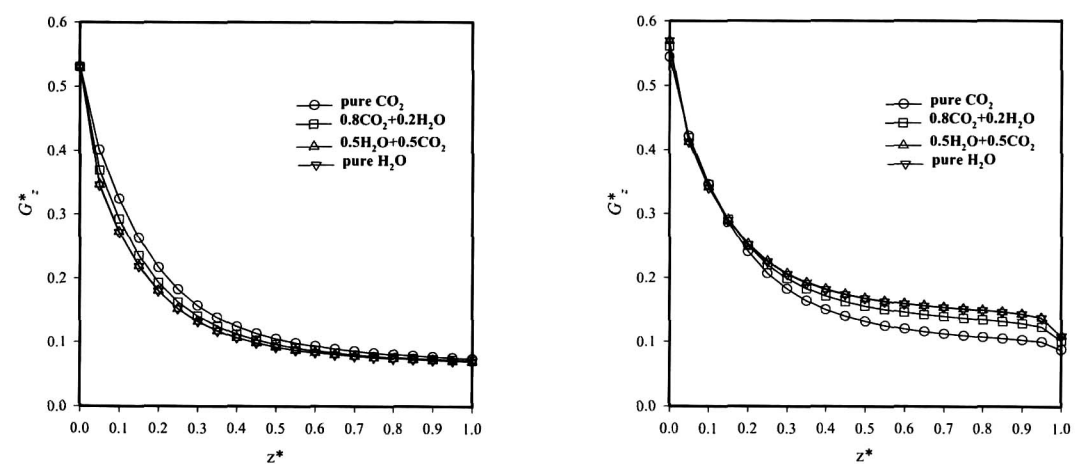

(a) $T_g = 0.5\,T_{hot}$ (b) $T_g = 0.7\,T_{hot}$

Fig. 5. Average intensity distributions for nongray gases (G^*_z at $r^* = 0.0$).

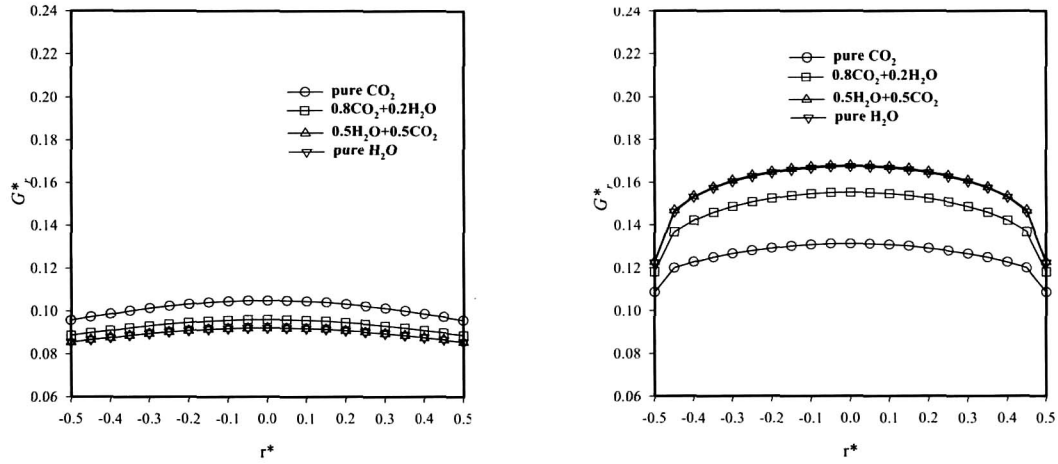

(a) $T_g = 0.5\,T_{hot}$ (b) $T_g = 0.7\,T_{hot}$

Fig. 6. Average intensity distributions for nongray gases(G_r^* at $z^* = 0.5$).

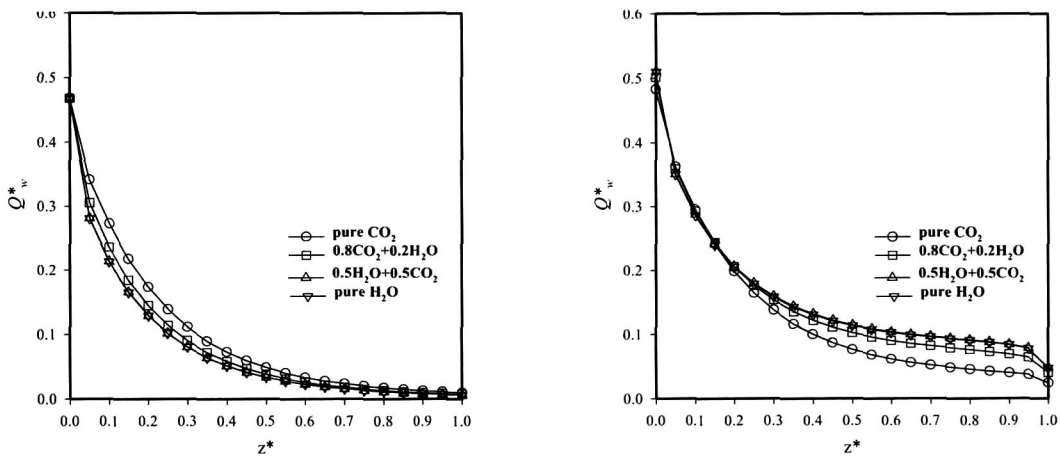

Fig. 7. Net side wall heat flux distributions for nongray gases(Q_w^* at $r^* = 0.5$).

The dimensionless net side wall radiative heat flux profiles(Q_w^*) are shown in Fig. 7 for different gas compositions. The side wall heat flux profiles are also affected by the gas compositions. For the low medium temperature of $T_g = 0.5T_{hot}$(Fig. 7a), higher CO_2 composition results in larger side wall heat fluxes due to the easy transmission of the radiative energy emitted from the bottom hot wall to the side wall. However, for the high medium temperature of $T_g = 0.7T_{hot}$(Fig. 7b), higher CO_2 composition results in smaller side wall heat fluxes due to the low radiative emission from the medium to the side wall.

Conclusions

In this paper we present some precise radiative transfer solutions for a black walled cylindrical system filled with purely absorbing gray and nongray gases where the medium is assumed to be uniform in properties and temperature. The solutions are obtained by using the ray tracing method with sufficiently accurate T_{95} quadrature set. The average radiative intensities and the radiative wall heat fluxes are obtained for gray gases with various absorption coefficients and for nongray gases with various compositions of the pure water vapor and the

pure carbon dioxide. Analytic exact values at various conditions are used to verify the gray gas results obtained from the numerical analyses, and the numerical solutions obtained from this study are very well matched with the exact values. Although the solution method used in this study is not suitable for engineering purposes, the resulting solutions can be used as the reference data in verifying the solution schemes for multidimensional radiative transfer. Numerical data including the average intensities and the radiative wall heat fluxes presented in this paper are avaliable through the author's internet site at

http://cau.ac.kr/~enegry/published/cylinder_nongray/data.html.

Acknowledgement

The authors wish to acknowledge the financial support of the Combustion Engineering Research Center (CERC).

References

1. Raithby, G.D. and Chui, E.H., 1990, "A Finite-Volume Method for Predicting a Radiant Heat Transfer in Enclosure with Participating Media," ASME J. Heat Transfer, Vol. 112, pp. 415-423.

2. Chui, J. C., Lee, H. S., and Patankar, S. V., 1994, "Finite Volume Method for Radiation Heat Transfer ", J. Thermophys. Heat Transfer, Vol. 8 No. 3, pp. 419-425

3. Cheung, K.B. and Song, T.H. 1997, "Discrete Ordinates Interpolation Method for Numerical Solution of Two-Dimensional Radiative Transfer Problems," Numercial Heat Transfer, Part B, Vol. 32, pp. 107-125.

4. Seo, S.H. and Kim, T.K., 1998, "Study on interpolation schemes of the discrete ordinates interpolation method for 3-D Radiative Transfer with Nonorthogonal Grids," ASME J. of Heat Transfer, Vol. 120, pp. 1091-1094.

5. Cha, H., Song, T-H, 2000, "Discrete Ordinates Interpolation Method Applied to Irregular Three-Dimensional Geometries," ASME J. Heat Transfer, Vol. 122, pp. 823-827.

6. Maruyama, S., and Aihara, T., 1995 "Radiative Heat Transfer of Arbitrary 3-D Participating Media with Non-participating Media by a Generalized Numerical Method REM", *Proc. 2nd Int'l. Symposium on Radiation Transfer*, Kusadasi, pp. 153-167

7. Maruyama, S., and Aihara, T., 1997 "Radiative Heat Transfer of Arbitrary Three-Dimensional Absorbing, Emitting and Scattering Media and Specular Diffuse Surface," ASME J. Heat Transfer, Vol. 119, pp. 129-136.

8. Liu, F., 1999, "Numerical solutions of Three-Dimension Non-Grey Gas Radiative Transfer Using the Statistical Narrow-Band Model," ASME J. of Heat Transfer, Vol. 121, pp. 200-203

9. Tae-Kuk Kim, Won-Hee Park and Chang-Hyung Lee, 2001, "Radiative Transfer Solutions for Pure Absorbing Gray and Nongray Gases within a Cubical Enclosure", KSME International Journal, Vol. 15 No. 6 pp. 752-763.

10. Thurgood, C.P., Pollard, A. and Becker, H.A., 1995 "The T_N Quadrature Set for the Discrete Ordinates Method," ASME Journal of Heat Transfer, Vol. 117, pp. 1068-1070.

11. Lockwood, F.C. and Shah, N.G., 1981, "A New Radiation Solution Method for Incorporation in General Combustion Predictions Procedure", in 18th Symposium on Combustion, The Combustion Institute, Pittsburg, PA, pp. 1405-1414.

12. Godson, W. L., 1953, "The evaluation of infrared radiation fluxes due to atmospheric water vapor," Quarterly Journal of Royal Meteorological Society, Vol. 79, pp 367-379.

13. Lindquist,G.H., Simmons, F.S., 1972, "A Band Model Formulation for Very Nonuniform Paths,"Journal of Quant. Spectrosc. Radiat. Transfer, Vol. 12, pp. 807-820

14. Zhang, L., Soufiani, A. and Taine, J., 1988, "Spectral Correlated and Noncorrelated Radiative Transfer in a Finite Axisymmetric System Containing an Absorbing and Emitting Real Gas-Particle Mixture," Int. J. of Heat and Mass Transfer, Vol. 31, pp. 2261-2272.

15. Ludwig, C.B., Malkmus, W., Readon, J.E. and Thompson, A.L., 1973, Handbook of Infrared Radiation from Combustion Gases, NASA SP-3080, Scientific and Technical Information Office, Washington D.C..

16. Soufiani A. and Taine J., 1997, High temperature gas radiative property parameters of statistical narrow-band model for H_2O, CO_2 and CO and correlated-k model for H_2O and CO_2," Int. J. Heat Mass Transfer, Vol. 4, No.4 pp987-991